

Sub-dekahertz Ultraviolet Spectroscopy of $^{199}\text{Hg}^+$

R. J. Rafac, B. C. Young,* J. A. Beall, W. M. Itano, D. J. Wineland, and J. C. Bergquist

National Institute of Standards and Technology, Boulder, Colorado 80303

(Received 8 May 2000)

Using a laser that is frequency locked to a Fabry-Pérot étalon of high finesse and stability, we probe the $5d^{10}6s^2S_{1/2}(F=0) \leftrightarrow 5d^96s^2D_{5/2}(F=2) \Delta m_F = 0$ electric-quadrupole transition of a single laser-cooled $^{199}\text{Hg}^+$ ion stored in a cryogenic radio-frequency ion trap. We observe Fourier-transform limited linewidths as narrow as 6.7 Hz at 282 nm (1.06×10^{15} Hz), yielding a line $Q \approx 1.6 \times 10^{14}$. We perform a preliminary measurement of the $5d^96s^2D_{5/2}$ electric-quadrupole shift due to interaction with the static fields of the trap, and discuss the implications for future trapped-ion optical frequency standards.

PACS numbers: 32.30.Jc, 06.30.Ft, 32.80.Pj, 42.62.Fi

Precision spectroscopy has held an enduring place in physics, particularly in the elucidation of atomic structure and the measurement of fundamental constants, in the development of accurate clocks, and for fundamental tests of physical laws. Two ingredients of paramount importance are high accuracy, that is, the uncertainty in systematic frequency shifts must be small, and high signal-to-noise ratio, since the desired measurement precision must be reached in a practical length of time. In this paper, we report the measurement of an optical absorption line in a single laser-cooled $^{199}\text{Hg}^+$ ion at a frequency $\nu_0 = 1.06 \times 10^{15}$ Hz (wavelength ≈ 282 nm) for which a linewidth $\Delta\nu = 6.7$ Hz is observed, yielding the highest $Q \equiv \nu_0/\Delta\nu$ ever achieved for optical (or lower frequency) spectroscopy. We also report a preliminary measurement of the interaction of the upper state electric-quadrupole moment with the static field gradients of the ion trap, which is expected to contribute the largest uncertainty for a frequency standard based on this system.

In spectroscopy and for clocks, fluctuations in frequency measurement are usually expressed fractionally: $\sigma_y(\tau) = \Delta\nu_{\text{meas}}(\tau)/\nu_0$, where τ is the total measurement time. When the stability is limited by quantum fluctuations in state detection, $\sigma_y(\tau) = C(2\pi\nu_0)^{-1}(N\tau_{\text{probe}}\tau)^{-1/2}$, where N is the number of atoms, τ_{probe} is the transition probe time (typically limited by the excited-state lifetime or the stability of the local oscillator), and C is a constant of order unity that depends on the method of interrogation. For many decades, the highest accuracies and the greatest stabilities have been achieved by locking a microwave oscillator to a hyperfine transition in an atomic ground state [1–5]. Since the fractional instability $\sigma_y(\tau)$ is inversely proportional to the transition frequency, greater stability can be attained using transitions at higher frequencies such as those in the optical region of the electromagnetic spectrum. Only recently have lasers of sufficient spectral purity become available to probe the narrow resonances provided by transitions between long-lived atomic states [6–12]. The stable laser source of Refs. [6,11] and the relative freedom from environmental perturbation afforded by ion trapping enable the high resolution reported here.

Combined with novel, highly compact, and accurate laser frequency measurement schemes [13,14], a trapped-ion optical frequency standard would appear to have significant advantages over present-day atomic clocks.

A partial energy-level diagram of $^{199}\text{Hg}^+$ is shown in Fig. 1. The 282 nm radiation used to drive the $2S_{1/2} \leftrightarrow 2D_{5/2}$ transition is produced in a nonlinear crystal as the second harmonic of a dye laser oscillating at 563 nm. The frequency of the dye laser radiation is electronically served to match a longitudinal mode of a high-finesse Fabry-Pérot cavity that is temperature controlled and supported on an isolation platform [6,11]. The stabilized laser light is sent through an optical fiber to the table holding the ion trap. Unavoidable mechanical vibration of this fiber broadens the laser spectrum by nearly 1 kHz. The fiber-induced phase noise is sensed and removed using a method [11] similar to that described in Ref. [15]. Finally, the frequency of the 563 nm light is referenced to the electric-quadrupole transition by first frequency shifting in an acousto-optic modulator (AOM) and then frequency doubling in a single pass through a deuterated ammonium dihydrogen phosphate crystal.

The design of the linear cryogenic ion trap used in these measurements borrows heavily from our previous work

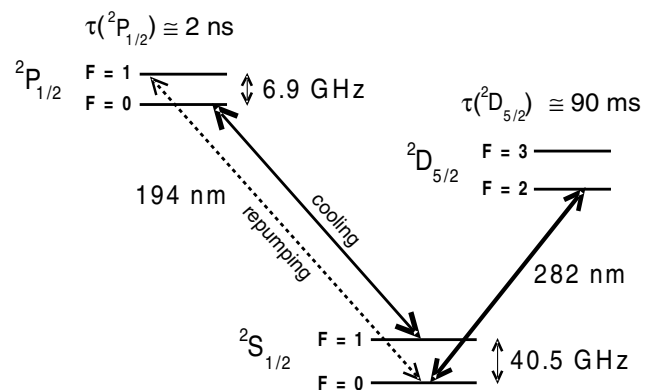


FIG. 1. Partial energy level diagram of $^{199}\text{Hg}^+$ with the transitions of interest indicated.

[4,16,17]. A single ^{199}Hg atom from a thermal source is ionized by an electron beam and trapped in the harmonic pseudopotential formed by the rf and static potentials of a linear quadrupole trap. The trap operates in analogy to a quadrupole mass filter having its ends “plugged” with static fields. The trap electrodes are constructed from Au-metallized alumina tubes 530 μm in diameter. The electrode axes are held parallel and coincident with the vertices of a square of side 1.37 mm by an alumina structure that facilitates electrical connection and mounting in the vacuum chamber.

One pair of diagonally opposite electrodes is segmented by laser micromachining prior to metallization to permit application of the axially confining static potential. The remaining pair of electrodes is driven by a cryogenic copper helical resonator coupled to a 8.6 MHz signal source. Under typical operating conditions, a single $^{199}\text{Hg}^+$ ion exhibits secular motion at 1.45, 1.86, and 1.12 MHz in the x , y , and z (axial) directions, respectively, as inferred from the vibrational sideband spectrum of the ion [18]. In addition, biasing electrodes are mounted outside the trap rods to cancel any stray static electric fields that may be present.

Previous experiments using ^{199}Hg were performed at room temperature and at a pressure of approximately 10^{-7} Pa [19]. Under those conditions, the background gas pressure was large enough that the ion would be lost due to chemical reaction after only a few minutes. To circumvent this, the ion trap is housed in a liquid He vacuum Dewar like that described in [17]. Engineering particulars of the liquid He cryostat allow low-frequency (<100 Hz) vibratory motion of the trap structure relative to the optical table. Uncorrected, these vibrations contribute 50–1000 Hz of Doppler broadening to the laser line. We eliminate the majority of this broadening using an additional stage of Doppler cancellation, where the correction signal is derived from optical heterodyne detection of a motion-sensing beam reflected from a mirror rigidly affixed to the trap [19]. The resulting cancellation is not ideal, because the sensing beam is steered by additional optical elements and its path deviates slightly from overlap with the probe beam near the trap. Measurements indicate that this optical path difference can contribute as much as 2 Hz to the spectral width of the 282 nm probe laser in the reference frame of the ion.

The ion is laser cooled to near the 1.7 mK Doppler limit by driving the $5d^{10}6s^2S_{1/2}(F=1) \leftrightarrow 5d^{10}6p^2P_{1/2}(F=0)$ cycling transition at 194 nm (Fig. 1) [18]. Because of weak off-resonant pumping to the $^2S_{1/2}(F=0)$ state, we employ a second 194 nm source phase locked to the first with a 47 GHz offset that returns the ion to the ground-state $F=1$ hyperfine level. We tolerate the complication of hyperfine structure, since only isotopes with nonzero nuclear spin can have first-order magnetic-field-insensitive transitions that provide immunity from fluctuations of the ambient field. This significantly relaxes the requirements for control and/or shielding of environmental magnetic sources.

We monitor the ion and deduce its electronic state using light scattered from the cooling transition. Fluorescence at 194 nm is collected by a five-element uv-grade fused silica $f/1$ objective located inside the cryostat. The scattered light is imaged outside the Dewar, spatially filtered with a 75 μm aperture, and relayed with a second lens to an imaging photomultiplier tube having $\approx 5\%$ quantum efficiency at 194 nm. Transitions to the $^2D_{5/2}$ state are detected using the technique of “electron shelving,” which infers the presence of the atom in the metastable level through the absence of scattering from the strong laser-cooling transition [18,20]. A metastable-state detection efficiency near unity can be achieved, because the absorption of a single 282 nm photon suppresses scattering of many photons from the 194 nm transition for a period determined by the lifetime of the $^2D_{5/2}$ state. The radiation from the 194 and 282 nm sources is admitted to the trap sequentially using mechanical shutters and an AOM, which prevents broadening of the quadrupole transition by the cooling radiation. Typical count rates are 2000 Hz for a single ion cycling at the half-power point of the cooling transition, compared to only 20 Hz combined laser scatter and photomultiplier thermal background when the ion is shelved in the metastable level.

Spectra of the recoilless “carrier” component of the $^2S_{1/2}(F=0) \leftrightarrow ^2D_{5/2}(F=2)$ $\Delta m_F=0$ transition were obtained for a range of probe times and laser intensities by laser cooling for 30 ms, preparing the ion in the $F=0$ ground state by blocking the repumping laser, and then interrogating the quadrupole transition. The spectra are built up from multiple bidirectional scans of the 282 nm probe laser frequency. Since the frequency drift of the probe laser is not precisely compensated, nor is it constant, we incorporate a locking step in between pairs of positive- and negative-going frequency sweeps about the center of the quadrupole resonance. In the locking sequence, we step the frequency of the probe laser alternately to the approximate half maximum on either side of the quadrupole resonance, probe for a fixed time τ_{servo} , and then look for transitions to the $^2D_{5/2}$ level. Typically, 48 measurements are made on each side of the resonance during each lock cycle. The asymmetry between the number of quantum jumps detected on the high- and low-frequency sides of the resonance is used to correct the frequency of a synthesizer used to compensate for cavity drift. In this fashion, variations in the frequency of the 282 nm laser for times exceeding several seconds are reduced. Using the locking step alone with $\tau_{\text{servo}} = 40$ ms, the error signal from the lock indicates a fractional frequency instability $\sigma_y(\tau) = 1.5 \times 10^{-15}$ for times comparable to the length of the combined servo and scanning cycle (15–60 s). This is worse than the quantum-projection-noise-limited stability ($\approx 5 \times 10^{-16}$) but is consistent with fluctuating quadratic Zeeman shifts arising from variations in the ambient magnetic field. The trap was not magnetically shielded during the measurements reported here.

Spectra are plotted in Fig. 2 for a variety of probe times $\tau_{\text{probe}} = 20$ –120 ms, with $\tau_{\text{servo}} = \tau_{\text{probe}}$. The

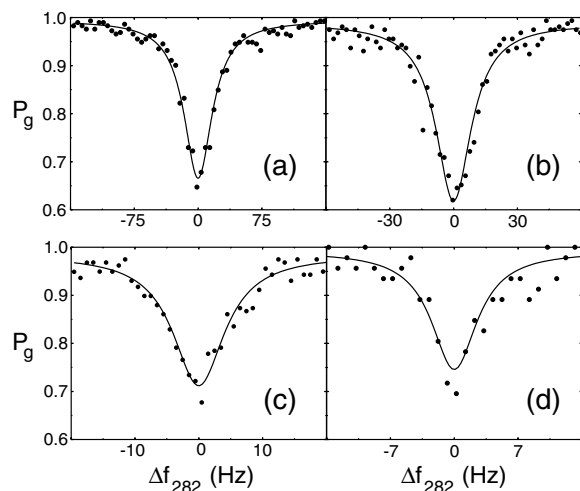


FIG. 2. Quantum-jump absorption spectra of the ${}^2S_{1/2}(F=0) \leftrightarrow {}^2D_{5/2}(F=2)$ $\Delta m_F = 0$ electric-quadrupole transition. Δf_{282} is the frequency of the 282 nm probe laser detuning, and P_g is the probability of finding the atom in the ground state. The four plots correspond to excitation with 282 nm pulses of different lengths: (a) 20 ms (averaged over 292 sweeps), (b) 40 ms (158 sweeps), (c) 80 ms (158 sweeps), and (d) 120 ms (46 sweeps). The linewidths are consistent with the Fourier-transform limit of the pulse at 40(2), 20(1), 10(1), and 6(1) Hz.

linewidths of all the spectra are transform limited by the finite probe time, decreasing to 6.7 Hz in the uv at 120 ms, the longest time used. The carrier transition amplitude is a function of the initial value of the vibrational quantum number n [see, for example, Eq. (31) of Ref. [21]]. Since for our trapping parameters $\langle n \rangle \approx 35$ at the Doppler cooling limit, it is not possible to transfer the electron to the ${}^2D_{5/2}$ state with unit probability. The observed signals are in good agreement with the theoretical expectation, and the signal loss for $\tau_{\text{probe}} = 120$ ms [Fig. 2(d)] is consistent with applying the probe for a time that exceeds the natural lifetime of the ${}^2D_{5/2}$ state by 33%. This result corresponds to a fractional frequency resolution of 6.3×10^{-15} , which we believe is the smallest reported for excitation with an optical or microwave source. The result is surpassed only by Mössbauer spectroscopy in ZnO, where a fractional linewidth of 2.5×10^{-15} was achieved using a nuclear source of 93 keV gamma rays [22], which is not practical for use in an atomic clock. The measurements reported here illustrate the potential of a single-ion optical frequency standard and confirm the phase stability of our probe laser system, validating the results of the heterodyne comparison of the two reference cavities [6,11]. An excellent review of the performance of similar systems can be found in Ref. [12].

Figure 3 shows a typical power-broadened spectrum with consequent Rabi “sidebands,” using $\tau_{\text{probe}} = 10$ ms and $\tau_{\text{servo}} = 40$ ms. A least-squares fit to the data indicates that it is consistent with a pulse area of $2.41(7)\pi$ (relative to $n \approx 0$) and a mean vibrational quantum number $\langle n \rangle = 73(9)$. This is twice the value of $\langle n \rangle$ expected at

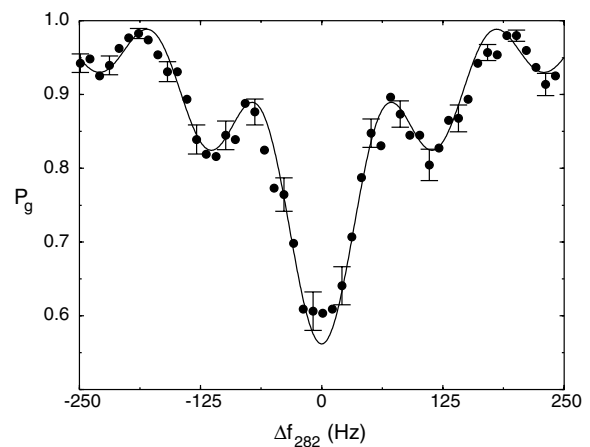


FIG. 3. Quantum-jump absorption spectrum of the power-broadened electric-quadrupole transition. Δf_{282} is the frequency of the 282 nm probe laser detuning, and P_g is the probability of finding the atom in the ground state. The data are averaged over 348 frequency sweeps with $\tau_{\text{probe}} = 10$ ms and $\tau_{\text{servo}} = 40$ ms. The solid line is a least-squares fit to a Rabi line profile with pulse area $2.41(7)\pi$ and $\langle n \rangle = 73(9)$. The quantum-projection-noise-limited uncertainty is indicated by representative error bars plotted every third point.

the Doppler cooling limit; the larger result is likely due to saturation of the cooling transition.

In Fig. 4 we plot the central three Ramsey fringes of a time-domain separated-oscillatory-fields interrogation of the ${}^2S_{1/2} \leftrightarrow {}^2D_{5/2}$ transition with 5 ms pulses separated by a 20 ms free-precession interval. In operation as a frequency standard, the Ramsey method offers $1.6\times$ reduction in linewidth (and a corresponding increase in stability) for an equivalent measurement period.

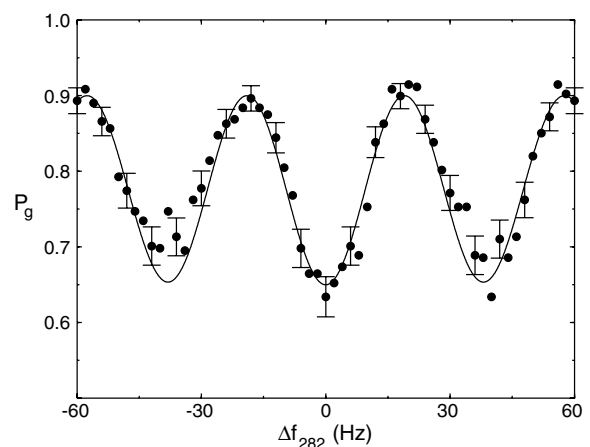


FIG. 4. The central three fringes obtained by time-domain Ramsey interrogation of the electric-quadrupole transition. Δf_{282} is the frequency of the 282 nm probe laser detuning, and P_g is the probability of finding the atom in the ground state. The data are averaged over 328 frequency sweeps with $\tau_{\text{servo}} = 40$ ms. The solid line is the expected Ramsey signal for 5 ms pulses separated by 20 ms of free precession; the $\approx 10\%$ background arises primarily from suboptimal setting of the discriminator levels in our detection electronics. The quantum-projection-noise-limited uncertainty is indicated by representative error bars plotted every third point.

It should be possible to reduce the uncertainties of all systematic shifts in this system including the second-order Doppler (time-dilation) shift and static or dynamic Zeeman and Stark shifts to values approaching 10^{-18} . The electric-quadrupole shift of the ${}^2D_{5/2}F = 2$ ($m_F = 0$) state arising from coupling with the static potentials of the trap is expected to be the limiting systematic contribution in future measurements of the absolute value of the ${}^2S_{1/2} \leftrightarrow {}^2D_{5/2}$ transition frequency, because of the difficulty in determining with certainty the magnitude and configuration of the static fields of the trap. In principle, it is possible to eliminate this shift by measuring the quadrupole transition frequencies for each of three mutually orthogonal orientations of a quantizing magnetic field of constant magnitude; the mean value is then the unperturbed ${}^2S_{1/2} \leftrightarrow {}^2D_{5/2}$ transition frequency. We follow this procedure for several values of the total magnetic induction and for all possible directions in a suitable coordinate system (e.g., $[1\ 1\ 1]$, $[1\ -1\ -1]$, $[-1\ -1\ 1]$, where $[1\ 1\ 1]$ is elevated 45° from the trap axis and 45° from the vertical plane). Using the ion as a magnetometer, the magnitude of the field produced by three sets of coils is calibrated by the measurement of the frequency of the $F = 0 \rightarrow 2$ ($\Delta m_F = 2$) magnetic field-dependent electric-quadrupole transition. For an ideal linear trap with secular frequencies $\omega_x = \omega_y$ and $\omega_z = 2\pi$ (1 MHz), we calculate a shift that varies between $+7.5$ and -15 Hz depending on field orientation. The estimate of the atomic quadrupole moment is based on Hartree-Fock wave functions for the ground state of Hg^+ , which yield the matrix element $\langle 5d|r^2|5d \rangle = 6.61 \times 10^{-21} \text{ m}^2$ [23]. In our apparatus we observe shifts departing from the mean frequency by $+12(7)$, $+9(13)$, and $-27(7)$ Hz for the three field orientations at 282 nm, in reasonable agreement with the simple model. The quoted uncertainties arise from imprecision in our ability to set the absolute magnitude and direction of the magnetic induction. Thus the fractional frequency uncertainty is of the order of 10^{-14} , and we might reduce this below 10^{-15} in the present apparatus with straightforward improvements to the magnetic shielding and control. Uncertainties approaching 10^{-18} should be obtainable through stringent control of magnetic fields in combination with a spherical rf quadrupole trap geometry that does not rely on static potentials for confinement. Greater resolution and accuracy might be more readily achieved using a different type of transition, e.g., the weak hyperfine-induced electric-dipole transitions like those between the low-lying 1S_0 and 3P_0 states of the singly ionized species of the Group IIIA elements of the periodic table [12,24,25], particularly in cases where first-order magnetic-field independent transitions are available (albeit at nonzero field) [26].

This research was partially supported by the Office of Naval Research and through a Cooperative Research and

Development agreement with Timing Solutions, Corp., Boulder, Colorado. We would like to thank C. Oates, J. Ye, and D. Sullivan for their careful reading of this manuscript.

*Present address: Jet Propulsion Laboratory, Pasadena, CA 91109.

- [1] A. Clairon *et al.*, in *Proceedings of the 5th Symposium on Frequency Standards and Metrology* (World Scientific, Singapore, 1996), pp. 49–59.
- [2] R. L. Tjoelker *et al.*, in *Proceedings of the 5th Symposium on Frequency Standards and Metrology* (Ref. [1]), pp. 33–38.
- [3] P. T. H. Fisk *et al.*, *IEEE Trans. Ultrason. Ferroelectr. Freq. Control* **44**, 344 (1997).
- [4] D. J. Berkland *et al.*, *Phys. Rev. Lett.* **80**, 2089 (1998).
- [5] S. R. Jefferts *et al.* (to be published).
- [6] B. C. Young *et al.*, *Phys. Rev. Lett.* **82**, 3799 (1999).
- [7] Ch. Salomon *et al.*, *J. Opt. Soc. Am. B* **5**, 1576 (1988).
- [8] N. M. Sampas *et al.*, *Opt. Lett.* **18**, 947 (1993).
- [9] O. Acef, *Opt. Commun.* **134**, 479 (1997).
- [10] S. Seel *et al.*, *Phys. Rev. Lett.* **78**, 4741 (1997).
- [11] B. C. Young *et al.*, in *Proceedings of the 14th International Conference Laser Spectroscopy* (World Scientific, Singapore, 1999), pp. 61–70.
- [12] A. A. Madej and J. E. Bernard, in “Frequency Measurement and Control,” edited by Andre N. Luiten, Springer Topics in Applied Physics (Springer-Verlag, Berlin, to be published).
- [13] J. Reichert *et al.*, *Phys. Rev. Lett.* **84**, 3232 (2000).
- [14] S. A. Diddams *et al.* (to be published).
- [15] L.-S. Ma *et al.*, *Opt. Lett.* **19**, 1777 (1994).
- [16] M. G. Raizen *et al.*, *J. Mod. Opt.* **39**, 233 (1992).
- [17] M. E. Poitzsch *et al.*, *Rev. Sci. Instrum.* **67**, 129 (1996).
- [18] J. C. Bergquist *et al.*, *Phys. Rev. A* **36**, 428 (1987).
- [19] J. C. Bergquist *et al.*, in *Frontiers in Laser Spectroscopy*, Proceedings of the International School of Physics “Enrico Fermi,” Course CXX (North-Holland, Amsterdam, 1994), p. 359.
- [20] H. G. Dehmelt, *Bull. Am. Phys. Soc.* **20**, 60 (1975); *J. Phys. (Paris) Colloq.* **42**, C8-299 (1980).
- [21] D. J. Wineland and W. M. Itano, *Phys. Rev. A* **20**, 1521 (1979).
- [22] G. J. Perlow *et al.*, *J. Phys. (Paris) Colloq.* **35**, C6-197 (1974).
- [23] A. D. McLean and R. S. McLean, *At. Data Nucl. Data Tables* **26**, 197 (1981).
- [24] H. G. Dehmelt, *IEEE Trans. Instrum. Meas.* **31**, 83 (1982).
- [25] E. Peik *et al.*, in *Proceedings of the 13th European Frequency and Time Forum and the 1999 IEEE Frequency Control Symposium, Besançon, France* (Institute of Electrical and Electronics Engineers, Piscataway, NJ, 1999), pp. 682–685.
- [26] D. J. Wineland and W. M. Itano, *Bull. Am. Phys. Soc.* **27**, 864 (1982).